LRP 564/96 December 1996

ITG-FREE TOKAMAK CONFIGURATIONS WITH MAGNETIC FIELD GRADIENT REVERSAL

M. Fivaz, T.M. Tran, K. Appert,
J. Vaclavik, S.E. Parker

submitted for publication in
Physical Review Letters

ITG-free tokamak configurations with magnetic field gradient reversal

M. Fivaz, T.M. Tran, K. Appert, J. Vaclavik, S.E. Parker[1]
Centre de Recherches en Physique des Plasmas, Association Euratom-Confédération Suisse, Ecole Polytechnique Fédérale de Lausanne, PPB, 1015 Lausanne, Switzerland.
[1] *Department of Physics, University of Colorado, Boulder, CO 80309, USA.*

Global gyrokinetic particle simulations have been used to search tokamak configurations which are stable against the Ion Temperature Gradient-driven (ITG) modes commonly held responsible for the core anomalous ion heat transport. The stable configurations are characterized by strongly reduced or reversed ∇B drifts on the low-field side. As in high β_p (poloidal beta) tokamak experiments excellent transport properties have been observed, we conjecture, inspired by our simulations, that this may be the result of the stabilization of ITG modes by the reduction of the ∇B drifts.

Ion Temperature Gradient-driven instabilities are now commonly held responsible for the turbulence giving rise to anomalous ion heat transport in the core of tokamaks; ITG-based transport models can successfully predict the plasma thermal transport over a wide range of parameters [1]. The reduction of this transport would be of great help to the achievement of a fusion reactor; configurations that are free of these instabilities are of very high interest. An effort has recently been made to find such configurations, e.g. oblate plasmas [2] and plasmas with sheared rotation [3] have been discussed as routes to ITG-mode stabilization. We propose here another route to ITG stability: the reduction of the ∇B drift on the low field side of the torus.

In this Letter, we study finite-pressure effects on ITG instabilities using the first global gyrokinetic Particle-In-Cell codes which work with full finite-pressure MHD equilibrium data. We note that microinstabilities in general equilibria were previously studied in the ballooning limit [4]. With respect to global ITG stability, we find that the dominant effect is related to the particle ∇B drift on the low field side of the torus: the growth rates decrease with decreasing ∇B drift. In fact, the configurations are stable when ∇B is close to reversal.

The ITG instability takes its free energy from the ion temperature gradient. It can be destabilized by the parallel motion (slab ITG), the poloidal magnetic drifts due to toroidicity (toroidal ITG) and the trapped-ion precession (trapped ion mode). The latter two destabilizing mechanisms are related to the magnetic drift,

$$\vec{v}_d = \frac{v_\parallel^2 + \frac{1}{2}v_\perp^2}{\Omega B^2}\vec{B} \times \nabla B + \frac{v_\parallel^2}{\Omega B^3}\vec{B} \times \mu_0 \nabla p, \tag{1}$$

where $\vec{B}$ denotes the magnetic field, Ω the ion cyclotron frequency, $v_\parallel$ and $v_\perp$ the parallel and perpendicular particle velocities, and p the plasma pressure. From a wave-particle interaction diagnostic implemented in one of our codes, we find that particles with $v_\perp >> v_\parallel$ contribute most to the instability. In a simple analysis which helps to understand the simulation results to be presented, the second term in eq. (1) can therefore be neglected. In the local, $k_\parallel = 0$, and fluid limits, the drift frequencies may then be defined as

$$\omega_d \;=\; nq\nabla\chi \cdot \vec{v}_d \;=\; \frac{nT_i}{e}\frac{\partial}{\partial\psi} ln B \qquad \text{and} \tag{2}$$

$$\omega^*_{Ti} \;=\; \frac{nq}{m_i\Omega}\sqrt{1-g^2}|\nabla\chi|\,|\nabla\psi|\frac{dT_i}{d\psi} \;=\; \frac{nT_i}{e}\frac{d}{d\psi} ln T_i, \tag{3}$$

where n is the toroidal mode number, e the electron charge, T_i the ion temperature, χ the straight field line poloidal angle, q the safety factor, $g = \nabla\chi\cdot\nabla\psi/(|\nabla\chi|\,|\nabla\psi|)$ and ψ the poloidal magnetic flux of the

equilibrium. Focusing on the toroidal ITG regime and taking the local and fluid limits of the gyrokinetic equation in the absence of a density gradient, one obtains the dispersion relation [5] [6]:

$$\omega^2 + \omega_{Ti}^* \omega_d = 0, \tag{4}$$

i.e. the mode is locally stable for $\omega_d > 0$ (favorable gradient region) and locally unstable for $\omega_d < 0$ (unfavorable gradient region), the growth rate increasing with $|\omega_d|$. Similar arguments can be made for trapped-particle-driven modes.

A direct way of stabilizing the mode is to lower the magnetic drift on the low-field-side of the torus, thereby reducing ω_d. In configurations where the magnetic field has a minimum, the ∇B drift is even reversed and the unfavorable gradient region is turned into a favorable gradient region. Figure 1 shows the contours of ω_d in two configurations: (a) the usual case of a low β_p equilibrium and (b) of a higher β_p equilibrium where the drifts are reversed over most of the plasma. The dashed region corresponds to negative values, i.e. the unfavorable gradient region. Configuration (a) has a wide region of unfavorable gradient and is expected to be unstable to global ITG modes. The configuration (b) has favorable gradients over most of the plasma and is expected to be stable to global modes.

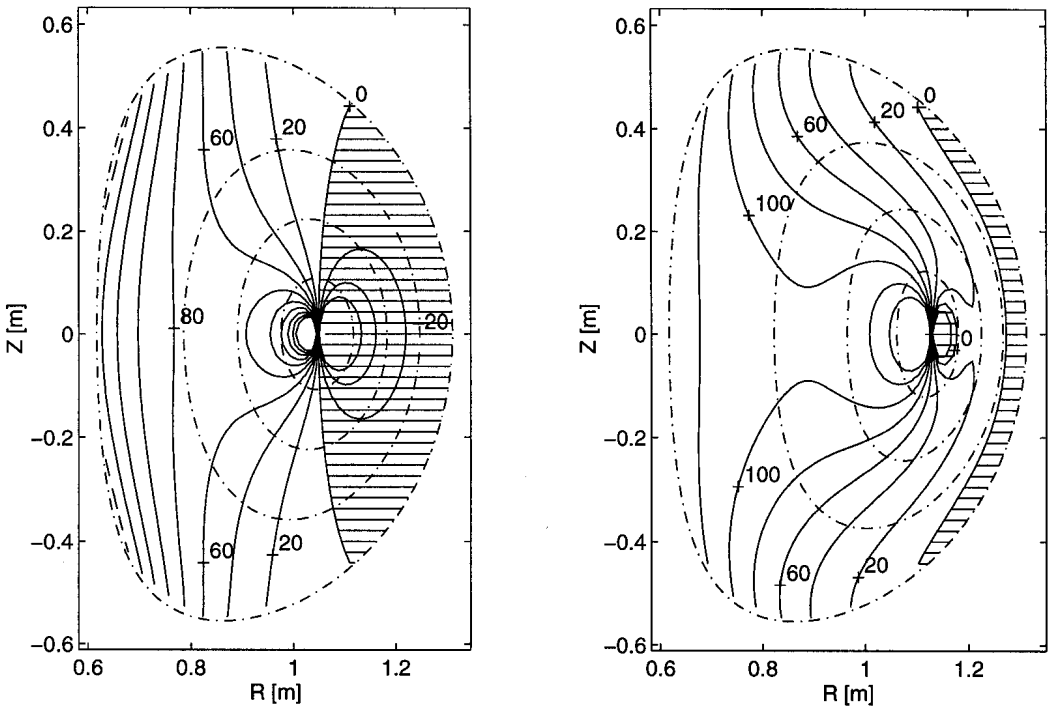

FIG. 1. Contours of the drift frequency ω_d (arbitrary units); the hatched zones correspond to negative values, i.e. to the unfavorable gradient region. The dashed lines correspond to the magnetic surfaces $s = 0.25$, $s = s_0$=0.5, $s = 0.75$ and $s = 1.0$. (a): standard configuration with $\beta = 3\%$ and local $\beta_p(s = s_0) = 1.2$. This configuration is unstable for ITG modes. (b): configuration with drift reversal on the low field side, $\beta = 4.4\%$, local $\beta_p(s = s_0) = 4.9$. This configuration is stable for all toroidal mode numbers.

In our simulations, the plasma is modeled with gyrokinetic ions [7] and adiabatic electrons. An axisymmetric equilibrium magnetic structure (solution of the Grad-Shafranov equation [8]) is provided by the MHD equilibrium code CHEASE [9]. The full plasma cross-section is considered in the simulations. We follow the time-evolution of electrostatic, quasineutral perturbations of a local Maxwellian equilibrium distribution function, using two different particle-in-cell (PIC) codes running on a massively parallel CRAY-T3D. The first one is a linear finite element PIC code [10] solving for the electrostatic potential in non-orthogonal magnetic coordinates and the second one is a new version of the nonlinear code ORB [11]. The latter works in cylindrical coordinates but has been modified [12] to accept the same MHD equilibrium data as the finite element code; here, it is used in its linear version only. Both codes give essentially the same results.

Other effects have been studied by many authors, e.g. electromagnetic perturbations [4] [13] and/or trapped electrons [14] [15]. Though their influence on our results will have to be investigated in future work, there are reasons to believe that the general conclusions will not be changed; we note, for instance, that the drives related to trapped electrons and to the ion physics are both determined by the radial gradient of the magnetic field. Furthermore, we focus here on flat density cases, where the effect of trapped electrons is expected to be small [16] [17].

A set of JET-shaped equilibria was produced, varying the sources (current and pressure profiles) in the Grad-Shafranov equation. The boundary shape and the value of the safety factor $q = 2$ at a given radial point, $s = s_0 = 0.5$, have been kept constant. Here, s is the square root of the normalized poloidal flux, $s = (\psi/\psi_0)^{0.5}$, and acts as the radial variable. Other parameters are: major radius $R_0 = .96$ m, minor radius $a = .35$ m, elongation $E = 1.6$, triangularity $\delta = 0.3$ and $B_0 = 1$ T. The set covers a wide range of parameters: $0 < \beta < 4.5\%$, $0 < \beta_p < 2.5$, shear $0.3 < \hat{s} < 0.9$ at $s = s_0$, internal inductance $0.5 < l_i < 1$ and Shafranov shift $0 < c < .5a$.

We then studied the stability of ITG modes in these equilibria, using a flat density profile, typical of the core of an H mode, and flat electron temperature $T_e = 1$ keV. The ion temperature profile was such that the logarithmic ion temperature gradient peaks at $s = s_0$, effectively confining the most unstable mode around $s = s_0$:

$$\frac{1}{T_i}\frac{dT_i}{ds} = -\kappa \cosh^{-2}\left(\frac{s - s_0}{\Delta s}\right), \tag{5}$$

where $\kappa = 1/0.35$, $\Delta s = 0.42$ and $T_i(s = s_0) = 1$ keV. As a consequence of these parameters one obtains $a/\rho_i = 76$ where ρ_i is the deuterium Larmor radius and $L_T/R_0 = 0.127$, where L_T is the temperature gradient scale length. The simulation provides the most unstable mode for a given toroidal mode number n.

The simulations confirm the simple analysis following eqs (2)-(4). The configuration (a) is unstable for several toroidal mode numbers n; the corresponding growth rates are shown in figure 2. The mode amplitudes peak in the negative ω_d region of unfavorable gradient. They are destabilized mainly by the poloidal magnetic drifts, but also somewhat by the parallel motion and the trapped ion precession, and thus can be classified as toroidal ITGs with small slab ITG and trapped-ion character.

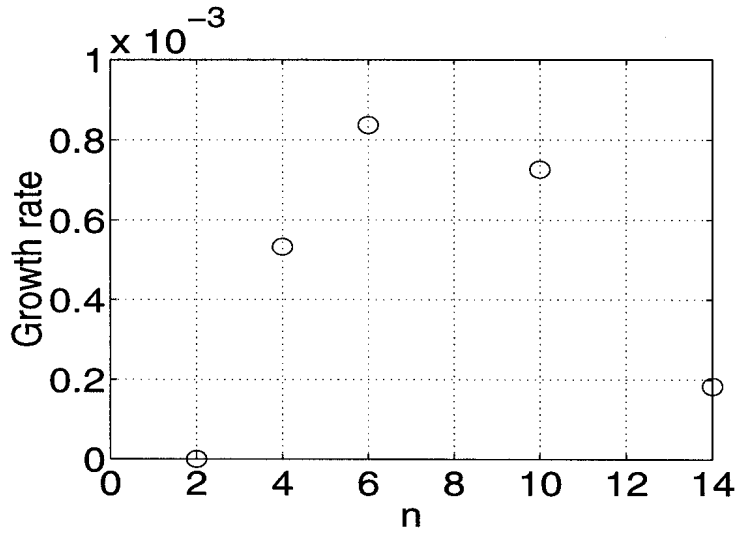

FIG. 2. Growth rate (normalized to the ion cyclotron frequency) as a function of toroidal mode number for the configuration (a) shown in figure 1.

The configuration (b) is found to be fully stable, i.e. stable for all values of n, despite the flat density ($\eta_i = \infty$) and the value of $L_T/R_0 = 0.127$ which usually lead to high growth rates [18]. This is because ∇B is favorable everywhere around $s = s_0$ where the ion temperature gradient is large. Note that a much stronger temperature gradient can give the mode a strong slab ITG character and therefore destabilize it despite the favorable gradient.

For further analysis, we restrict ourselves to the surface $s = s_0$, and define $\epsilon = -\omega_d/\omega^*_{Ti}$, its local value on the low field side of the mid-plane ϵ_t and its magnetic surface average

$$\langle\epsilon\rangle = \frac{\oint \epsilon\, dl/B}{\oint dl/B}. \tag{6}$$

We note that ω^*_{Ti} is a magnetic surface quantity and commutes with the surface average in $\langle\epsilon\rangle$. Let us consider the usual model configurations with circular concentric magnetic surfaces and with $B \sim 1/R$, where R is the distance from the axis of symmetry. In such a case, ϵ_t is the standard parameter quantifying toroidicity in the ballooning limit and is equal to L_T/R_0. The ITG growth rate has a maximum with respect to ϵ_t [18]. The positive (favorable gradient) and negative (unfavorable gradient) contributions from ω_d almost cancel each other and $\langle\epsilon\rangle \approx 0$. This is in contrast to the situation in drift-reversed equilibria where the average has only positive contributions and $\langle\epsilon\rangle$ is of the order 1 and positive. Figure 3 shows the growth rate of the n=6 mode of all the configurations studied versus the average drift frequency ratio $\langle\epsilon\rangle$. The correlation between the two quantities is almost perfect for $\langle\epsilon\rangle > 0.2$. The values of $\langle\epsilon\rangle < 0.2$ have lower growth rates than at $\langle\epsilon\rangle$=0.2; they correspond to equilibria where ϵ_t is large but where ϵ averages close to zero and where, similarly to the model configuration results [18], ϵ_t is above the value that leads to the highest growth rate.

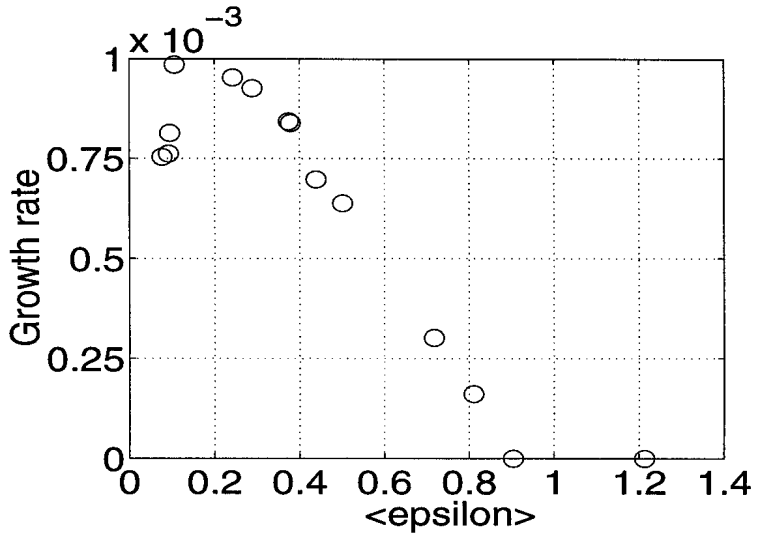

FIG. 3. Growth rate (normalized to the ion cyclotron frequency) of the $n = 6$ mode for different configurations, as a function of the surface-averaged drift frequency ratio $\langle\epsilon\rangle =< -\omega_d/\omega^*_T >$ at $s = s_0$.

We found that $\langle\epsilon\rangle$ is in fact the best indicator for ITG stability, but two other quantities come near. The first is the traditional MHD magnetic well [19] which is also a measure for the surface average of ∇B and shows excellent correlation with the growth rate [10]. Similar conclusions were drawn in [20] for purely trapped particle modes. The second is the local (at $s = s_0$) value of β_p which is related with ∇B drift reduction through the gradient of the toroidal magnetic field. In contrast, the growth rates do not correlate well with the global value of β_p, nor with parameters such as the shear at $s = s_0$, the Shafranov shift, the internal inductance l_i, or the normalized plasma pressure β.

There are a number of experimental discharges in various devices where the stabilization of microinstabilities by the reduction of ∇B may have contributed to a reduction of anomalous transport. As the ∇B drift reduction tends to occur in equilibria with high local (i.e. local to a magnetic surface) values of β_p [8] these equilibria should have relatively high global β_p as well. In several tokamaks, some high β_p discharges, when free of ELMs, have indeed shown very good confinement properties. On JET [21] and DIII-D [22], confinement substantially better than the JET/DIII-D H-mode scaling has been obtained. On PBX-M [23], the heat diffusivity was seen to decrease in time while β_p increased. On JT-60U [24] [25] [26], high β_p discharges showed a highly enhanced confinement leading to record-breaking neutron yields; the ion heat transport was found to be low everywhere in the core unlike the situation when a H-mode transport barrier is present. This is consistent with a stabilization of microinstabilities by the reduction of ∇B over a wide radial extension.

A preliminary analysis of JET equilibria with low current and relatively high β_p (≈ 1.5) has shown that a reduction of ∇B by a factor of four (compared to a usual, low-beta configuration with $B \sim 1/R$) can experimentally be realized. In such conditions, a drastic reduction of ITG-induced transport is expected. Detailed studies of the transport properties of such discharges should be undertaken concentrating on cases without gross MHD activity (ELMs and sawteeth).

A condition for drift reversal can be derived by noting that the unfavorable gradient occurs in the region where $\frac{\partial B}{\partial \psi} < 0$. Using the equation of MHD equilibrium $\mu_0 \nabla p = (\nabla \times \vec{B}) \times \vec{B}$, one can easily show that, for an axisymmetric system,

$$B \frac{\partial B}{\partial \psi} = -\frac{1}{R} \frac{\partial R}{\partial \psi} B_t^2 - \mu_0 \frac{dp}{d\psi} + 0(B_p^2), \tag{7}$$

where B_t and B_p are the toroidal and poloidal components of the magnetic field. The $0(B_p^2)$ term on the right-hand side of this equation is small compared to the first one and may be neglected. Thus drift reversal occurs when

$$-\mu_0 \frac{dp}{d\psi} > \frac{1}{R} \frac{\partial R}{\partial \psi} B_t^2, \tag{8}$$

i.e. the pressure gradient must be sufficiently large. Note that large pressure gradients can destabilize MHD modes; configurations of practical interest might have to compromise between microstability and MHD stability.

In conclusion, we have presented global gyrokinetic PIC simulations which show that ITG modes can be stabilized by a reduction of the equilibrium ∇B drifts. For fixed plasma shape, safety factor at half radius and ion temperature gradient, ITG stability is determined by these drifts. We expect similar tendencies for other magnetic-drift-driven microinstabilities such as collisionless trapped particle modes. We find that, for relatively strong gradients ($L_T/R_0 = 0.127$), a configuration is fully ITG stable when the ∇B drifts are close to reversal. Such magnetic configurations do exist in some experimental discharges and should, according to our simulations, be characterized by a low level of ITG transport. We also conjecture that the experimentally observed low level in ELM-free high-β_p discharges may be due or partly due to reduced ∇B drifts on the low-field side.

In the near future, a serious effort should be made in analyzing experimental data from MHD-quiescent discharges, trying to correlate ∇B reduction with ion thermal transport. On the theory side, the future search for stable configurations should not be limited to microstability but must include MHD considerations as well.

This research was supported in part by both the Cray/EPFL Parallel Application Technology Program and the Swiss National Science Foundation. All computations have been performed on the Cray-T3D of the Ecole Polytechnique Fédérale in Lausanne. We acknowledge useful discussions with S. Brunner, F. Hofmann, L. Villard and H. Weisen from CRPP as well as help with experimental data analysis from B. Balet, W. Heidbrink, G. Huysmans and W. Zwingmann from JET.

---

[1] M. Kotschenreuther, W. Dorland, M. A. Beer, and G. W. Hammett, Phys. Plasmas **2**, 2381 (1995).
[2] M. Kotschenreuther and W. Dorland, private communication, 1996.
[3] M. Artun, W. M. Tang, and G. Rewoldt, Phys. Plasmas **2**, 3384 (1995).
[4] G. Rewoldt, W. M. Tang, and M. S. Chance, Phys. Fluids **25**, 480 (1982).
[5] X. Garbet *et al.*, Phys. Fluids B **4**, 136 (1992).
[6] F. Romanelli, Phys. Fluids B **1**, 1018 (1989).
[7] T. S. Hahm, Phys. Fluids **31**, 2670 (1988).
[8] J. Wesson, *Tokamaks* (Clarendon Press, Oxford, 1987).
[9] H. Lütjens, A. Bondeson, and O. Sauter, Comput. Phys. Commun. **97**, 219 (1996).
[10] M. Fivaz *et al.*, in *Theory of fusion plamas, Int. Workshop, Varenna, August 1996* (Editrice Compositori, Societa Italiana di Fisica, Bologna, 1997).
[11] S. E. Parker, W. W. Lee, and R. A. Santoro, Phys. Rev. Letters **71**, 2042 (1993).
[12] T. M. Tran *et al.*, Int. Sherwood Fusion Theory Conf., Philadelphia, March 1996, book of abstracts 2C21, 1996.

[13] M. Kotschenreuther, G. Rewoldt, and W. M. Tang, Comp. Phys. Comm. **88**, 128 (1995).
[14] M. Beer, Ph.D. thesis, Princeton University, 1996.
[15] R. D. Sydora, V. K. Decyk, and J. M. Dawson, to be published in Plasma Physics and Controlled Fusion.
[16] G. Rewoldt and W. M. Tang, Phys. Fluids B **2**, 319 (1990).
[17] W. W. Lee and W. M. Tang, Phys. Fluids **31**, 612 (1988).
[18] J. Q. Dong, W. Horton, and J. Y. Kim, Phys. Fluids B **4**, 1867 (1992).
[19] J. P. Freidberg, in *Ideal Magnetohydrodynamics* (Plenum, New York, 1987), Chap. 6.
[20] M. Rosenbluth and M. L. Sloan, Phys. Fluids **14**, 1725 (1971).
[21] C. D. Challis *et al.*, Nuclear Fusion **33**, 1097 (1993).
[22] P. A. Politzer *et al.*, Phys. Plasmas **1**, 1545 (1994).
[23] B. LeBlanc *et al.*, Nuclear Fusion **33**, 1645 (1993).
[24] T. Nishitani *et al.*, Nuclear Fusion **34**, 1069 (1994).
[25] M. Mori *et al.*, Nuclear Fusion **34**, 1045 (1994).
[26] Y. Kamada *et al.*, Nuclear Fusion **34**, 1605 (1994).